Normal reference values for left atrial strains and strain rates in school children assessed using two-dimensional speckle-tracking echocardiography

日本大学医学部小児科学系小児科学分野

神保　詩乃

申請年　2020 年

指導教員　森岡　一朗

Heart and Vessels
https://doi.org/10.1007/s00380-020-01594-0

ORIGINAL ARTICLE

Normal reference values for left atrial strains and strain rates in school children assessed using two-dimensional speckle-tracking echocardiography

Shino Jimbo[1] · Nobutaka Noto[1] · Hirotsugu Okuma[1] · Masataka Kato[1] · Akiko Komori[1] · Mamoru Ayusawa[1] · Ichiro Morioka[1]

Received: 26 November 2019 / Accepted: 27 March 2020

Abstract

Left atrium (LA) function is a known predictive marker of heart failure in adults. Few reports of LA function analyses using LA strain (ε) and strain rate (SR) measurements in children exist. Thus, this study aimed to determine normal reference values for LA ε and SR in healthy school children and to investigate methods of interpreting LA function data based on maturational changes using two-dimensional speckle-tracking echocardiography (2DSTE). We recruited 112 healthy school children (median age 12.0 years; range 6–16 years). LA ε and SR were investigated using 2DSTE multi-vendor analysis software (TomTec Imaging Systems, Germany) and compared to Doppler parameters and LA volumes measured by the conventional method. The onset of the P wave was selected as the reference point for the LA ε analysis. Normal ranges of LA ε [reservoir (εRS), conduit (εCD), or contractile (εCT)] and positive SR (SR_{POS}), early negative SR (SR_{EN}), and late negative SR (SR_{LN}) were obtained using *Z*-score models via the lambda-mu-sigma method. According to the *Z*-score curves, all ε showed slight falling or continuous flat lines against age, body surface area (BSA), or heart rate (HR); however, ε CT showed modestly positive associations with HR. As for SR, the *Z*-score curves showed falling lines against age and BSA. In contrast, *Z*-score curves for SR_{EN} and SR_{LN} showed rising lines against HR. SR_{EN} was independent of E/e' and was negatively correlated with LA volume indexed against BSA. This study demonstrated the normal reference values for LA ε and SR using 2DSTE in school children. The present results recommended that LA ε should be evaluated together with changes in LA SR for accurate assessment, considering maturational changes including age, BSA, and HR in school children.

Keywords Left atrial function · Left atrial strain · Left atrial strain rate · Left atrial volume · Two-dimensional speckle-tracking echocardiography

Introduction

The left atrium (LA) plays an important role in the left ventricle (LV) performance throughout the cardiac cycle. The LA works as a reservoir during ventricular systole and isovolumic relaxation, a conduit that manages flow from the pulmonary veins to the ventricle during early diastole, and has an active role in the cardiac cycle by contracting during late diastole (Fig. 1). Doppler echocardiographic indices (trans-mitral LV inflow velocities and tissue Doppler mitral annular velocities) are well-known and useful parameters for grading diastolic dysfunction. Recently, several reports have demonstrated that three-dimensional speckle-tracking echocardiography (3DSTE) can derive complicated LA geometry precisely and reproducibly [1, 2]. The normal values and maturational changes using 3DSTE have been reported previously [1]. Even if 3DSTE becomes popular for LA analysis, the clinical practicality of two-dimensional speckle-tracking echocardiography (2DSTE) remains unchanged. Computed tomography (CT) and magnetic resonance imaging (MRI) are also able to measure LA function; however, they are limited by their temporal resolution [3]. Because 2DSTE is easy to perform during a short period of time and has a good temporal resolution, it could be appropriate for pediatric analyses. LA strain (ε) using 2DSTE has been

✉ Shino Jimbo
shino.jimbo@nihon-u.ac.jp

1 Department of Pediatric and Child Health, Nihon University School of Medicine, 30-1 Ohyaguchi-kamicho, Itabashi-ku, Tokyo 173-8610, Japan

Published online: 11 April 2020

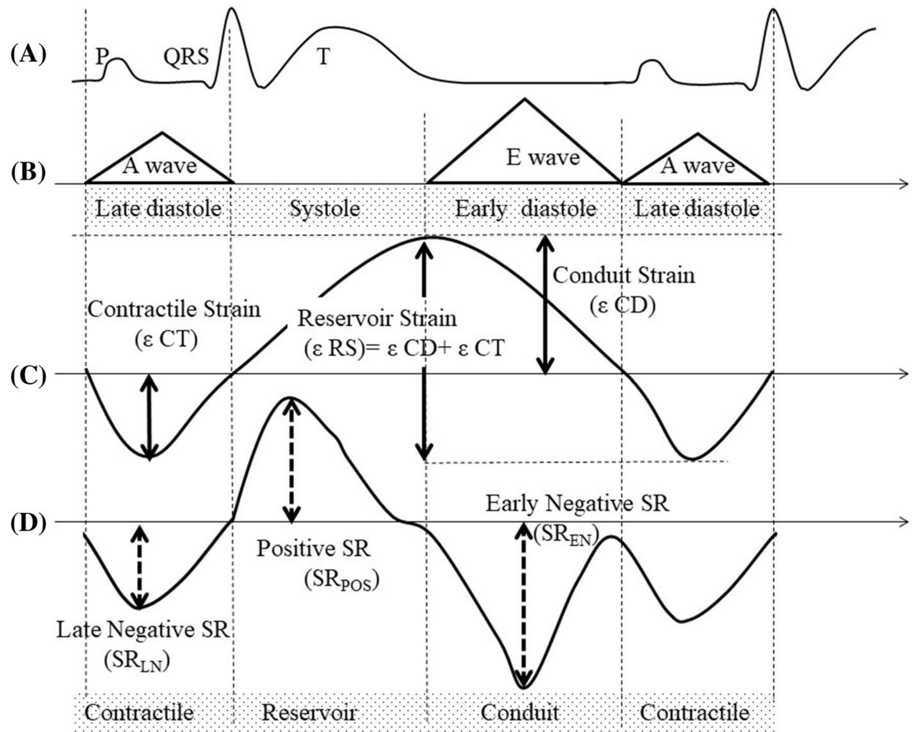

Fig. 1 Schematic representation of LA functions during the cardiac cycle. **a** ECG. **b** Transmitral Doppler flow velocity profiles. **c** LA strain curve. **d** LA strain rate curve. *εCD* conduit strain, *εCT* contractile strain, *εRS* reservoir strain, *SR* strain rate, SR_{EN} early negative strain rate, SR_{LN} late negative strain rate, SR_{POS} positive strain rate

reported to be a predictive marker of cardiac events with good reproducibility [4–7]. Many validated studies reported that LA *ε* showed sensitive changes in LV diastolic dysfunction preceding LA volume enlargement [4–6]. LA remodeling due to atrial fibrillation causes changes in LV compliance [8] and LA *ε* [2]. In addition, its capacity to screen LA thrombus has been recently reported [7].

Currently, normal reference values for the three components of LA function have been demonstrated in adults [9–12]. However, this method has not yet been validated in children, and the volume of data are inadequate to determine the normal range of the LA *ε* and strain rate (SR). Moreover, whether LA function assessed by 2DSTE can be applied to children as well as adults because its interpretation depends on age, body surface area (BSA) or heart rate is unclear [13]. Thus, this study aimed (1) to report the normal reference values for LA *ε* and SR in healthy school children and (2) to investigate methods of interpreting LA functions according to maturational changes using 2DSTE.

Materials and methods

Subjects

This was a cross-sectional single-center trial conducted from May 2016 to December 2017. We recruited 153 patients (age range 6–16 years) who were screened for heart murmur, nonspecific chest pain, and palpitation. They were investigated if their medical history and physical examination results indicated that they were free of cardiac disease. We excluded 13 patients (8.4%) who were found to have heart disease ($n=7$) or abnormal ECGs ($n=6$) after cardiac screenings. The data of the remaining 140 patients with normal echocardiographic findings were included. Demographic and echocardiographic parameters were collected. Blood pressure was measured in the supine position at the beginning of the echocardiography. BSA was calculated using the DuBois formula [14]. The research protocol was approved by our institutional ethics committee, and the requirement for informed consent was waived on the condition that the project opt-out was disclosed on the internet (RK-171212-07).

Echocardiography

Studies were performed using Artida (CANON Medical Systems, Tochigi, Japan) at high frame rates (mean 93.5 ± 21 frames/s) using a 2.5–5 MHz transducer. All 2D data sets were able to be obtained without sedation. Left ventricular (LV) ejection fraction (LVEF) was calculated in the apical four-chamber view using the biplane modified Simpson's method and the diameter of the LV outflow tract (LVOT) was measured in the parasternal long-axis view in mid-systole. In the apical four-chamber view, peak *E* (early diastolic filling) and A (late diastolic filling) wave velocities were recorded from the LV inflow waveforms obtained during pulsed-Doppler echocardiography. Tissue Doppler imaging was used to measure the lateral mitral annular velocity (*E*′).

The mitral annular plane systolic excursion (MAPSE) was extracted from the lateral mitral annulus by M mode echocardiography in the same view. Pulsed-Doppler interrogation of time-velocity integrals (VTI) in the LVOT was manipulated while maintaining the beam axis at an angle that was as close as possible to parallel with the LVOT flow in the apical five-chamber view. Stroke volume (SV) was estimated using the following formula [15]:

$$\text{SV} = \text{Cross-sectional area of the LVOT } \left(\text{cm}^2\right) \times \text{LVOT VTI (cm)}$$

LA volumes were measured using the biplane-area-length method. Maximum LA volume (LAV max) and minimum LA volume (LAV min) were calculated in the apical four- and two-chamber views at ventricular end-systole and end-diastole, respectively [16]. These values were corrected according to each patient's BSA [left atrial volume index (LAVI max) and minimum left atrial volume index (LAVI min)].

All Doppler measurements were averaged over three consecutive cardiac cycles to account for respiratory variation in accordance with the ASE guidelines [17].

Echocardiographic imaging and 2DSTE analysis

Two-dimensional image clips of five consecutive cardiac cycles (as raw data) obtained from the apical four-chamber view were acquired in the Digital Imaging and Communications in Medicine format for further analysis. The following precautions were taken to acquire good LA images: (1) to ensure inclusion of the LA wall, the image was obtained in the left lateral recumbent position; (2) to optimize endocardial definition, the gain was set at a slightly higher level; (3) to maintain an identical frame rate and heart rate (HR), the depth and sector size were controlled, thus reducing the amount of information that needed to be processed. As for those children who were able to hold their breath, images were acquired during the end-expiratory phase with holding breath. LA ε and SR were analyzed offline using 2D software (2D Cardiac Performance Analysis, TomTec Imaging system, Munich, Germany). The LA was visualized as shown in Fig. 2a. Three points (septal and lateral corners of the mitral annulus and LA roof) were plotted manually using a point-and-click technique followed by automatic tracing of the endocardial LA borders. The epicardial line was the region of interest which was divided into three regions as follows: lateral wall, medial wall, and roof. The atrial appendage and pulmonary veins were excluded from the LA cavity. The image quality was visually checked using animation. We excluded the subjects if we could not track all segments, and we modified the method to retrace any segments not tracked in any part of the endocardial LA wall to obtain good images. The global longitudinal LA ε curve was displayed, which was set to start at the beginning of the QRS wave by default. The most suitable cardiac cycle was chosen for analysis and was set to change the reference point of the trigger as the P wave (Fig. 2b). Based on the LA volume curve which was derived simultaneously, the marker of end-systole (eS) was moved to the maximum LA cavity and the marker of end-diastole (eD) was shifted to the beginning of the P wave on the ECG. Because the P trigger was adopted as the calculation for LA ε, asymmetric sinusoidal curves with two peaks were recorded. The first negative peak and the second positive peak were measured as the contractile ε (ε CT: atrial contraction) and conduit ε (ε CD: LV filling), respectively. The reservoir ε (ε RS) was calculated as the sum of these two strains. Each of the three segments and an average of these SR curves were measured at the same time (Fig. 2c). SR in late diastole (SR_{LN}), ventricular systole (SR_{POS}), and early diastole (SR_{EN}) were measured along the average SR curve as the parameters of contractile, reservoir, and conduit function, respectively. Three consecutive cardiac cycles were analyzed in each data set, and the mean of these measurements was used for further analysis to minimize random error.

Intraobserver and interobserver variability

The intraobserver agreements, interobserver agreements, and test–retest variability were assessed using intraclass correlation coefficients (ICC) in 20 randomly selected subjects. The parameters of LA volume, LA ε, and SR were re-measured by the same observer over 1 month after the initial evaluation and a second observer performed the same measurements on separate occasions without knowledge of the results of the first observer. To determine test–retest variability, 2D data sets acquired by the same methodology were reanalyzed 1 h after the initial study.

Statistical analysis

All continuous data are presented as means ± standard deviations (SD) or as median with interquartile ranges if it shows skewed distribution. The categorical variables are expressed in percentages. The Kolmogorov–Smirnov test was used to check the normal distribution of the variables. Normally distributed continuous data were compared with the unpaired Student's *t* test and the continuous data with skewed distribution were assessed by Mann–Whitney *U* test for statistical significance. To compare the LA strains and the pulsed-Doppler echocardiographic indices or LA volumes, Pearson's correlation coefficient was used for data with normal distributions and Spearman's correlation coefficient was used for data with skewed distributions.

Comparisons of clinical characteristics and echocardiographic parameters, along with LA ε and SR among the

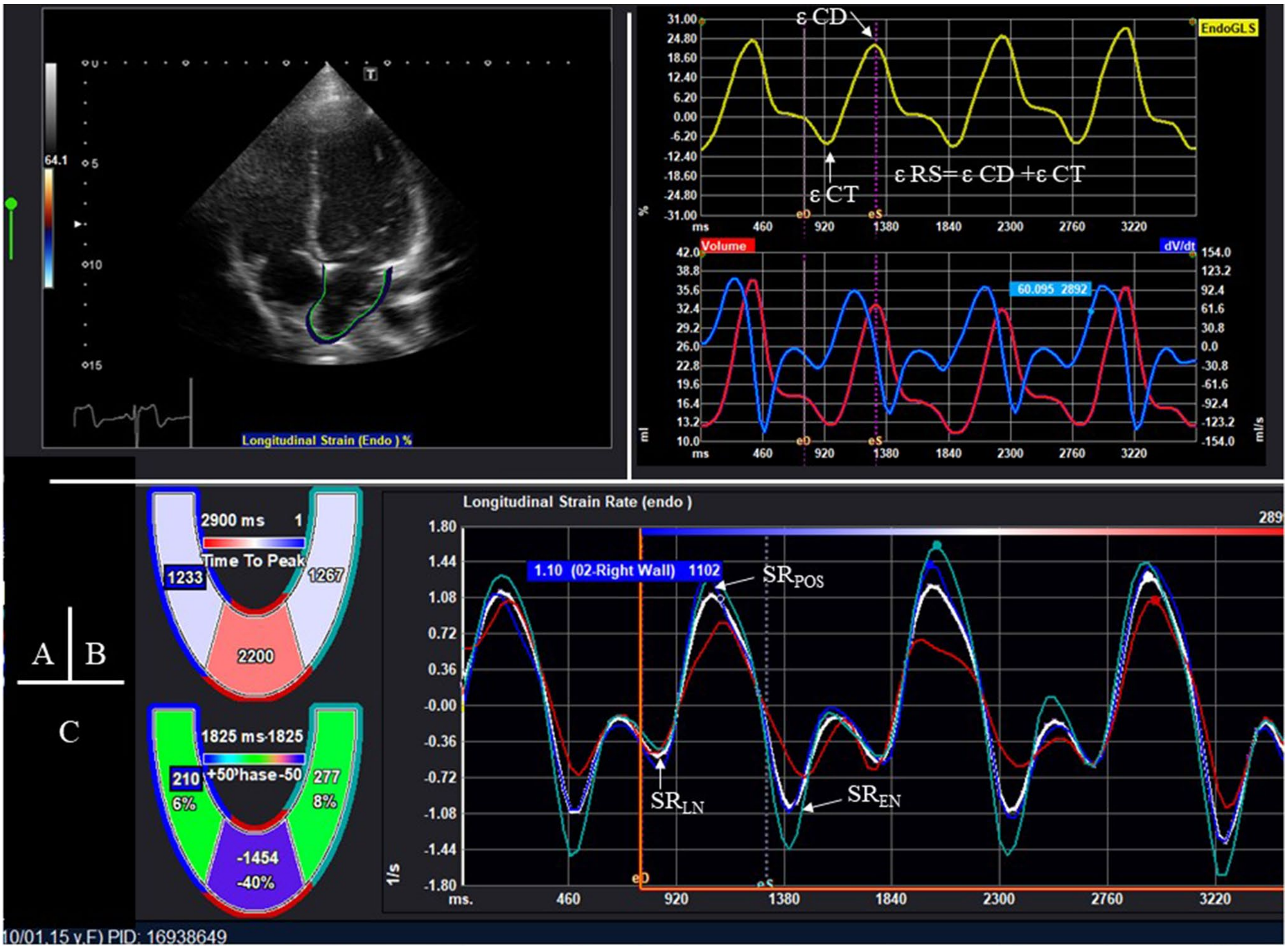

Fig. 2 LA functional analysis using the 2D speckle tracking method obtained from an apical four-chamber view. **a** Two-dimensional images obtained from the apical four-chamber view were acquired for analysis. Three points (septal and lateral corners of the mitral annulus and LA roof) were plotted manually using a point-and-click technique followed by automatic tracing of the endocardial LA borders. The epicardial line was created as the region of interest which was divided into the following regions: lateral wall, medial wall, and roof. (**b**, Top) the LA global strain (yellow line) curve. (**b**, Bottom) the LA volume curve (red line). To match the phase of the cardiac cycle, the end systole line was fixed to the maximum LA volume along the LA volume curve. The end diastole line was set to the beginning of the P wave as P trigger. The blue line shows the derived LA volume with respect to time. **c** The strain rate (SR) for each segment was obtained. The longitudinal average strain rate is shown on the white line

three age groups, were analyzed using a one-way analysis of variance (ANOVA) for normally distributed data or Kruskal–Wallis test for data with skewed distribution. In this study, the lambda-mu-sigma (LMS) method was used for the description of pediatric anthropometric data, allowing the calculation of percentiles and accurately normalized *Z*-scores and accounting for nonlinearity and a skewed distribution of reference data sets [18]. The LMS method describes the distribution of the measurement *Y* by its median (*M*), the coefficient of variation (*S*), and a measure of skewness (*L*) required to transform the data to normality, and the *Z*-score is calculated as follows:

$$Z\text{-score} = \{[Y/M(t)]L(t) - 1\}/[L(t) \times S(t)].$$

In this equation, *Y* is the individual LA strain measurement, and *L*, *M*, and *S* originate from the specific reference values for age, BSA, and HR (*t*), respectively. We describe the *Z*-score curves for each LA strain with lines indicating the − 2.5, − 2.0, − 1.0, 0, 1.0, 2.0, and 2.5 SD boundaries (corresponding to the 0.6, 2.3, 15.9, 50.0, 84.1, 97.7, and 99.4 percentiles, respectively). Detailed methods for developing the LMS models were previously reported [19]. The model with the lowest Akaike information criterion value was selected as the best model. Data analyses and calculations were performed using commercially available software, EZR (Saitama Medical Center, Jichi Medical University, Saitama, Japan) [20] and R version 3.4.0 (The R Foundation for Statistical Computing Vienna, Austria). A *p* value < 0.05 was considered statistically significant.

Table 1 Clinical and echocardiographic characteristics of the study populations ($n=112$)

Variables	Value
Age (years)	13 [10–14]
Male (%)	52 (46.4)
Height (cm)	153.9 [140.2–162.4]
BW (kg)	42.5 ± 12.7
BSA (m^2)	1.3 ± 0.3
HR (beats/min)	69.0 ± 11.8
Systolic BP (mmHg)	107.6 ± 10.2
Diastolic BP (mmHg)	61.2 ± 7.8
LVEF (%)	79.0 ± 5.3
Mitral *E*/*A*	1.8 ± 0.4
Mitral *E*/*e′*	5.7 ± 1.3
MAPSE (mm)	16.1 ± 2.4
SVI (ml/m^2)	43.8 ± 8.1
LAVI max (ml /m^2)	25.4 ± 3.9
LAVI min (ml/ m^2)	9.8 ± 2.6

Data are expressed as mean ± SD, median [interquartile range] or *n* (%)

BSA body surface area, *BP* blood pressure, *HR* heart rate, *LAVI max* maximum left atrial volume indexed to BSA, *LAVI min* minimum left atrial volume indexed to BSA, *LVEF* Left ventricular ejection fraction, *MAPSE* mitral annular plane systolic excursion, *SVI* stroke volume indexed to BSA

Results

LA ε and SR measurements were obtained from 140 patients; however, measurements of 28 patients were eliminated due to poor echocardiographic image quality. The final study population included 112 patients (median 12.0 years, range 6–16 years). Their demographic and echocardiographic data are shown in Tables 1, 2 and 3. There were no sex-specific differences in age, BSA, HR, LA ε, or LA SR.

Table 4 summarizes the correlations between each strain parameters and pulsed-Doppler indices or LA volumes. Among the pulsed-Doppler index results, the *E*/*A* ratio showed that a modest negative correlation with SR_{LN}. *E*/*e′* was negatively correlated with ε RS and ε CD. No significant association was observed between *E*/*e′* and the three SR. MAPSE was positively correlated with ε RS, ε CD, and SRpos respectively ($p<0.01$, $r=0.36$, 0.36, 0.32, respectively). SR_{EN} was modestly correlated with the stroke volume index (SVI) and LAVI max or LAVI min ($p=0.02$, $r=-0.21$, -0.22, -0.22, respectively). SR_{LN} was modestly correlated with the LAVI min ($p<0.01$, $r=-0.24$).

The *Z*-score curves are shown in Fig. 3. With increasing age and BSA, the three ε showed slightly falling lines or flat lines. The three SR also showed a negative correlation with these parameters, and these slopes were steeper than those of

Table 2 Clinical characteristics and reference value of echocardiographic parameters by age groups

Variables	Age			*P* value
	6–9 years ($n=25$: M13/F12)	10–12 years ($n=28$: M14/F14)	13–16 years ($n=59$: M25/F34)	
Age (years)	8 [7, 8]	12 [11, 12]	14 [13, 14]	< 0.01*
Height (cm)	126.1 [121.0–134.6]	151.0 [145.2–154.3]	161.0 [156.1–166.6]	< 0.01*
BW (kg)	26.1 ± 6.0	40.5 ± 8.4	50.3 ± 9.0	< 0.01*
BSA (m^2)	0.96 ± 0.1	1.3 ± 0.2	1.51 ± 0.1	< 0.01*
HR (beats/min)	77.4 ± 10.7	72.5 ± 12.4	63.7 ± 9.0	< 0.01*
Systolic BP (mmHg)	101.7 ± 9.3	107.2 ± 10.1	110.4 ± 9.6	< 0.01*
Diastolic BP (mmHg)	57.8 ± 7.1	62.3 ± 7.4	62.2 ± 7.9	0.04*
LVEF (%)	79.3 ± 5.3	78.2 ± 5.8	79.2 ± 5.1	0.67
Mitral E/A	1.7 ± 0.4	1.7 ± 0.4	1.9 ± 0.4	0.25
Mitral *E*/*e′*	5.9 ± 1.7	5.6 ± 1.3	5.8 ± 1.1	0.61
SVI (ml/ m^2)	40.4 ± 6.8	44.4 ± 8.4	44.9 ± 8.2	0.06
MAPSE (mm)	14.8 ± 2.5	16.4 ± 2.4	16.5 ± 2.2	< 0.01*
LAVI max (ml/m^2)	22.5 ± 4.6	25.9 ± 3.5	26.4 ± 3.2	< 0.01*
LAVI min Total (ml/ m^2)	8.5 ± 2.1	10.4 ± 3.0	10.1 ± 2.5	0.02*

BSA body surface area, *BP* blood pressure, *F* female, *HR* heart rate, *LAVI max* maximum left atrial volume indexed to BSA, *LAVI min* minimum left atrial volume indexed to BSA, *LVEF* left ventricular ejection fraction, *M* male, *MAPSE* mitral annular plane systolic excursion, *SVI* stroke volume indexed to BSA

*Statistically difference among groups. Data are expressed as mean ± SD or median [interquartile range]

Table 3 Reference value of LA ε and SR parameters by age groups

Variables	Age			*P* value
	6–9 years (*n* = 25: M13/F12)	10–12 years (*n* = 28: M14/F14)	13–16 years (*n* = 59: M25/F34)	
ε RS (%)	34.5 ± 7.8	34.5 ± 8.6	31.3 ± 7.5	0.10
ε CD (%)	26.0 ± 7.6	26.0 ± 9.0	23.7 ± 7.1	0.31
ε CT (%)	− 8.6 ± 2.9	− 8.5 ± 2.8	− 7.6 ± 2.6	0.19
SR_{POS} (S^{-1})	1.3 ± 0.3	1.2 ± 0.3	1.1 ± 0.3	0.03*
SR_{EN} (S^{-1})	− 1.7 ± 0.5	− 1.3 ± 0.4	− 1.2 ± 0.3	< 0.01*
SR_{LN} (S^{-1})	− 0.7 [− 0.8 to − 0.6]	− 0.5 [− 0.6 to − 0.4]	− 0.5 [− 0.6 to − 0.4]	< 0.01*

ε CD conduit strain, *ε CT* contractile strain, *ε RS* reservoir strain, *F* female, *M* male, *SR_{EN}* early negative strain rate, *SR_{LN}* late negative strain rate, *SR_{POS}* positive strain rate

*Statistically significance among groups. Data are expressed as mean ± SD or median [interquartile range]

Table 4 Correlations of LA strains (ε) and strain rate (SR) with Doppler echocardiographic indices and LA volumes

	LA ε: *r* (*p*)			SR: *r* (*p*)		
	ε RS	ε CD	ε CT	SR_{POS}	SR_{EN}	SR_{LN}
E/*A*	0.08 (0.43)	0.07 (0.42)	0 (0.98)	0.13 (0.19)	0.03 (0.76)	− 0.2 (0.04) *
E/*e′*	− 0.21 (0.03)*	− 0.20 (0.03)*	− 0.02 (0.82)	0.02 (0.82)	− 0.01 (0.9)	− 0.13 (0.19)
SVI	− 0.06 (0.55)	− 0.06 (0.56)	0 (0.94)	− 0.17 (0.07)	− 0.21 (0.02) *	− 0.14 (0.15)
MAPSE	0.36 (< 0.01)*	0.36 (< 0.01)*	0.01 (0.94)	0.32 (< 0.01)*	− 0.09 (0.36)	− 0.07 (0.48)
LAVI max	− 0.03 (0.72)	− 0.07 (0.50)	0.08 (0.38)	0 (0.98)	− 0.22 (0.02) *	− 0.04 (0.66)
LAVI min	− 0.13 (0.16)	− 0.1 (0.28)	− 0.1 (0.3)	− 0.18 (0.06)	− 0.22 (0.02)*	− 0.24 (< 0.01) *

Pearson's correlation coefficient or spearman's rank correlation coefficient *Statistically different

ε CD, ε CT, and SR_{LN} are expressed as absolute values

LAVI max maximum left atrial volume indexed to BSA, *LAVI min* minimum left atrial volume indexed to BSA, *MAPSE* mitral annular plane systolic excursion, *SVI* stroke volume indexed to BSA

ε. In the part of higher HR, SR_{EN} and SR_{LN} were more likely to have higher values. The ε CT showed the same tendency. However, ε RS, ε CD, and SR_{POS} were less affected by the change in HR.

The reproducibility of LA volume, LA strains, and SR is shown in Table 5. All parameters showed good favorable agreement; however, the LAV min had the lowest interobserver variability.

Discussion

In this study, we demonstrated the normal reference values for LA ε and SR in healthy school children using vendor-independent 2DSTE software (TomTec), which was developed for the LA analysis in this study. To the best of our knowledge, no previously published data exist on the normal reference values of the three components of LA ε and SR using *Z*-score models in this age range.

Previous studies

To date, there have been three published reports about the normal range of LA ε and SR in children [1, 13, 21]. According to these works, ε RS was affected by age; one study reported that LA ε increased with age [21] and the other showed controversial results [1]. This might have been caused by differences in the modality or LA analysis software, which is still an issue when interpreting LA ε and SR. In this study, we could show that εRS did not increase with age and that it decreased slightly in this cohort using 2D vendor-independent software. Moreover, there seemed to be a drastic change of LA ε and SR at the younger age group especially in children below 5 years old [13]. Even if HR variability was reported to affect LA ε and SR, it is unknown whether this trend could be explained only by the maturational change. For these reasons, we excluded the younger age group (younger than 5 years) including neonates from this study because of the difficulty in obtaining good images for analysis and because fluctuation may occur even without sedation.

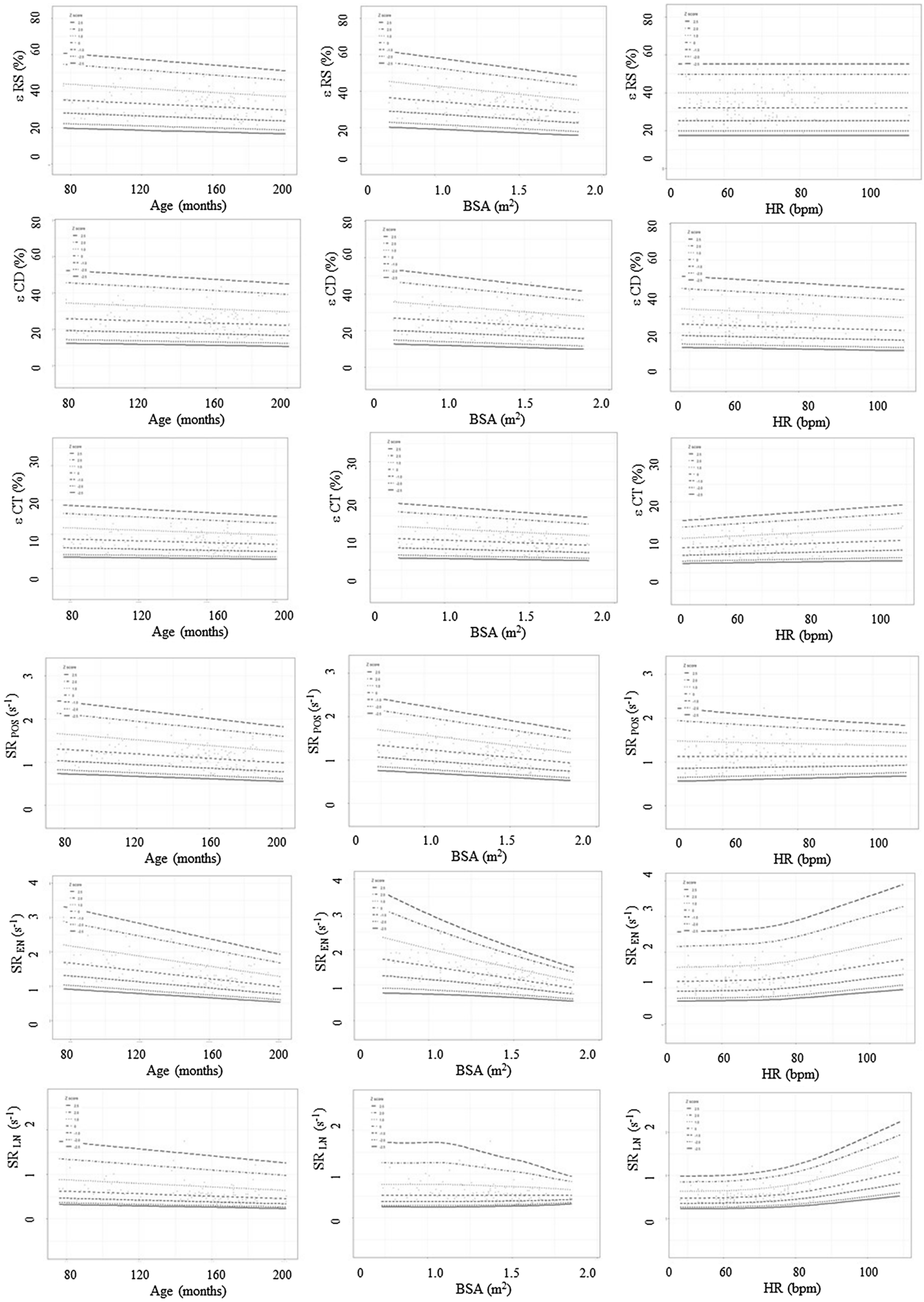

Fig. 3 *Z*-score curves of the LA *ε* and SR using the LMS models based on age, BSA, and HR. *BSA* body surface area, *HR* heart rate, *LA* left atrium, *LMS* lambda-mu-sigma. Z-score curves for each LA strain and SR with lines indicate the − 2.5, − 2.0, − 1.0, 0, 1.0, 2.0, and 2.5 standard deviation (SD) boundaries, respectively

Table 5 Intraclass correlation coefficients of the LA volume, LA strain (ε), and LA strain rate (SR)

Variable	Intraobserver		Interobserver		Test–retest	
	ICC	95% CL	ICC	95% CL	ICC	95% CL
LAV max	0.969	0.926–0.988	0.900	0.765–0.959	0.952	0.856–0.985
LAV min	0.889	0.746–0.954	0.711	0.406–0.874	0.741	0.361–0.912
ε RS	0.921	0.771–0.975	0.869	0.626–0.958	0.937	0.814–0.98
ε CD	0.882	0.671–0.962	0.834	0.538–0.946	0.898	0.709–0.967
ε CT	0.849	0.589–0.951	0.797	0.454–0.934	0.84	0.571–0.948
SR_{POS}	0.917	0.759–0.974	0.832	0.55–0.945	0.870	0.625–0.956
SR_{EN}	0.899	0.713–0.968	0.791	0.456–0.931	0.879	0.661–0.961
SR_{LN}	0.848	0.588–0.951	0.809	0.483–0.938	0.804	0.49–0.935

CL confidence limits, *ε CD* conduit strain, *ε CT* contractile strain, *ε RS* reservoir strain, *ICC* intraclass correlation coefficients, *LAV max* maximum left atrial volume, *LAV min* minimum left atrial volume, SR_{EN} early negative strain rate, SR_{LN} late negative strain rate, SR_{POS} positive strain rate

There were several matters of concern about the LA ε and SR measurements, and LA ε was reported as a useful parameter when evaluating cardiac dysfunction in children with atrial septal defect [22], valve aortic stenosis [23], Kawasaki disease [24], and diseases that cause LA enlargement [25]. Even in complex heart structures, strains have been reported as a sensitive marker of single ventricle function after the Fontan procedure during follow-up [26, 27]. Additionally, the possibility of their clinical applicability for monitoring the health of obese children [28] and athletes [29] has been reported. Our study showed that SR had a better temporal resolution than ε. Furthermore, ε has been reported that to respond to loading conditions to some extent [30, 31]; however, it would be useful to evaluate the deformation of the myocardium in the age group in which HR could be kept constant. On the contrary, our study might suggest that SR would be a suitable parameter for the assessment of the younger age group which would show a higher HR with great maturational changes. To apply the LA mechanics of children in clinical use, continuous assessments of LA ε and LA SR are crucial. The three SR segments were not validated in this study; however, their values may enable a better understanding of the adaptation of LA function [32]. Future studies are needed to evaluate these parameters in detail.

There are many reports on the measurement of the phasic LA volume curve using the 2DSTE method [33–37]. Notably, it enabled the volume-based assessment of LA function, which correlated with the conventional Doppler parameters, ε, and SR in the same phases of the cardiac cycle. A good correlation was found between the data obtained by 2DSTE and manual trace [33, 36]; however, LA volume derived from 2DSTE has been reported to be greater than that derived from the biplane area-length method because of the extra inclusion of entry sites of pulmonary veins as a part of the left atrium [37]. Therefore, LA volume was assessed by the biplane area-length method in our study, according to the ASE guidelines [16].

Parameters affected by LA ε and SR

The LA ε and SR cannot be discussed without consideration of the maturational changes of the LA myocardium. A matter of concern is what factor is most affected by LA ε or SR. All ε and SR in this population showed less influence on age. As for BSA, the *Z*-score curves of three LA ε showed weak downward slopes with leveling off. These trends were similar to those of age, while SR_{EN} and SR_{LN} were decreased with increasing BSA, and this finding may suggest that SR would have a tendency to be influenced by HR. In this study, we were able to evaluate the effects of HR on LA ε and SR in the groups which were expected to have relatively small fluctuations with age and BSA. SR_{POS} and all LA ε, except ε CT were less influenced by HR. In contrast, SR_{EN} and SR_{LN} significantly increased with increased HR. The reason why ε CT, SR_{EN}, and SR_{LN} were influenced by HR was that these parameters reflected mainly in diastole and tachycardia would shorten the cardiac cycles more in diastole than in systole. Careful interpretation of SR values considering HR is needed in further study. Although healthy school children were recruited for our study, we should consider afterload and preload, which are affected by volume status in addition to maturational changes when evaluated in children with heart disease. According to a previous study that reported the cut-off value for discriminating healthy children from those with juvenile cardiomyopathies, $\varepsilon RS \geq 40.4\%$ (sensitivity, 98%; specificity, 99%) and $SR_{pos} \geq 1.39\ s^{-1}$ (sensitivity, 88%; specificity, 90%) were optimal [38]. Maturational factors were not considered throughout that study; however, both values were between $Z+0$ and $Z+1.0$ in our study. Further studies are needed to determine the cutoff on this *Z* score curve.

Application of LA analysis

A consensus is lacking regarding if a practical algorithm for grading diastolic function in adults could be applied to children with congenital and acquired heart disease [39]. Some validated reports, which organized the pulsed-Doppler and tissue Doppler velocities in children are useful [39–41]; however, these have limitations regarding angle and volume dependence. Moreover, the correlation between LVEDP and these parameters are reportedly weak [42] and its tendency is more remarkable in LV systolic dysfunction [43], because they are easily affected by LV motion. Therefore, many researchers have been seeking the optimal parameters to improve the diagnostic accuracy of the diastolic dysfunction in children [25, 44]. 2DSTE could be one of the diagnostic tools for assessing LA phasic function although many potential confounders like age, BSA, or HR are unavoidable with pediatric echocardiography. We hope that this method would facilitate the assessment of diastolic function in the pediatric field, which may lead to favorable management of heart disease in the future by combining it with conventional pulse-Doppler parameters.

Two issues should be discussed for the application of LA analysis in children. First, the zero-reference point in the LA analysis can be determined in two ways. In our study, we selected the P wave as a reference point because the ε CT was derived more clearly with the P trigger compared to the R trigger. Some authors have indicated that the P trigger is more suitable than the R trigger when analyzing the LA strain because the R wave peak represents the electrical signal associated with LV contraction, which is not the same as the point at which minimum LA volume should be measured [45]. This gap might affect children more because of their relatively higher HR. Second, there is still no consensus as to whether 2D or 3D should be chosen for the LA analysis. The analyses using 3DSTE obtain full volumes of images precisely, rapidly, and with good reproducibility compared to 2DSTE [2]. Moreover, its characteristics make it possible to evaluate not only the longitudinal strain but also the circumferential strain [1, 2]. On the contrary, the strength of 2DSTE is its high temporal resolution, which could allow for the analysis of rapid events, such as the isovolumic phases and diastole when evaluating children with tachycardia [10]. Practically, the 2D analysis does not require short periods of breath-holding to obtain adequate images, which is sometimes a challenge for children when taking 3D images.

Modelling of child growth data

In our study, we chose the LMS method to derive the *Z*-score curve of LA ε and SR in children. This method has become standard for the modeling of child growth data [46] and has been adopted by the Centers for Disease Control and Prevention (CDC) for assessing growth. Until now, growth charts were established based on the cross-sectional data; however, the LMS method can be transformed to normalize the actual resource using Box–Cox power, and it avoids bias by regression to the mean. We searched for and finally selected the minimum Akaike information criterion for each model to avoid overfitting models in this study. Generally, the statistical power relies on the sample size, and the LMS method is not an exception to this rule. Recently, the Gaussian process regression (GPR) method has been reported to detect *Z*-scores with good accuracy compared to the LMS method in children [47]. In future studies, GPR with a sufficient population larger than the one used for this study needs to be investigated to determine a better prediction model.

Study limitations

We acknowledge the limitations of our study. First, there was a relatively small number of participants, and only those of certain ages were involved in the study. This might have influenced the correlations between age, BSA, and HR and LA ε or SR. We intended to recruit sufficient sample sizes for each age range based on the study design to derive the *Z*-score curve; however, many images had to be omitted from the study because of low image quality and insufficient information regarding the echocardiographic Doppler parameters. This was a retrospective single-center study; therefore, sampling bias might have been introduced. Moreover, we recognized that we should establish the normal value of the younger age group in a future study, as this was not determined in this study. Second, there were actually a few subjects of the younger age group whose image acquisition could not be performed during the end-expiratory phase. Both LA ε and SR can be affected by respiration with increased LA volume during inspiration, secondary to negative intrathoracic pressure. As respiration influences preload for the left atrium, average data were used for analysis; however, the variation related to respiratory cycles was inevitable. Third, the 2DSTE method generally requires appropriate machine settings to obtain the desirable quality of the 2D images based on frame rate, grayscale, depth of field, the region of interest, and timing of initial onset (P wave or QRS wave). Although difficulties with machine settings cause limitations in normal reference value comparisons, the analysis of LA functions using 2DSTE is expected to promote a better understanding of LA mechanics. This is the first study to use vendor-independent 2D software to determine the normal range of strain and SR in the LA of young children. Therefore, we expect that the results could help echocardiography experts working in various centers to validate their data.

Conclusion

We provided normal reference values for the three components for LA ε and SR in children using a *Z*-score model derived by the LMS method. The measurements of LA ε and SR using the 2DSTE method were easy to perform with good reproducibility. There were small maturational changes in LA ε that were probably clinically irrelevant. However, the LA SR should be evaluated together with changes in LA ε for precise evaluation of LA dysfunction, in consideration of maturational changes including age, BSA, and HR. Future studies will need to collect data from a greater number of healthy children and adolescents for clinical use.

Acknowledgements We thank Masashi Mikami, MS, for his statistical support with the *Z*-score models.

Compliance with ethical standards

Conflict of interest The authors declare that they have no conflict of interest.

References

1. Ghelani SJ, Brown DW, Kuebler JD, Perrin D, Shakti D, Williams DN, Marx GR, Colan SD, Geva T, Harrild DM (2017) Left atrial volumes and strain in healthy children measured by three-dimensional echocardiography: normal values and maturational changes. J Am Soc Echocardiogr 31:187–193
2. Mochizuki A, Yuda S, Oi Y, Kawamukai M, Nishida J, Kouzu H, Muranaka A, Kokubu N, Shimoshige S, Hashimoto A, Tsuchihashi K, Watanabe N, Miura T (2013) Assessment of left atrial deformation and synchrony by three-dimensional speckle-tracking echocardiography: comparative studies in healthy subjects and patients with atrial fibrillation. J Am Soc Echocardiogr 26:165–174
3. To AC, Flamm SD, Marwick TH, Klein AL (2011) Clinical utility of multimodality la imaging: assessment of size, function, and structure. JACC Cardiovasc Imaging 4:788–798
4. Brecht A, Oertelt-Prigione S, Seeland U, Rücke M, Hättasch R, Wagelöhner T, Regitz-Zagrosek V, Baumann G, Knebel F, Stangl V (2016) Left atrial function in preclinical diastolic dysfunction: two-dimensional speckle-tracking echocardiography-derived results from the BEFRI trial. J Am Soc Echocardiogr 29:750–758
5. Singh A, Addetia K, Maffessanti F, Mor-Avi V, Lang RM (2017) LA Strain For Categorization of LV diastolic dysfunction. JACC Cardiovasc Imaging 10:735–743
6. Xu TY, Sun JP, Lee AP, Yang XS, Ji L, Zhang Z, Li Y, Yu CM, Wang JG (2015) Left atrial function as assessed by speckle-tracking echocardiography in hypertension. Medicine (Baltimore) 94(6):e526
7. Zhu MR, Wang M, Ma XX, Zheng DY, Zhang YL (2018) The value of left atrial strain and strain rate in predicting left atrial appendage stasis in patients with nonvalvular atrial fibrillation. Cardiol J 25:87–96
8. Uetake S, Maruyama M, Mitsuishi T, Takahashi K, Miyauchi Y, Seino Y, Shimizu W (2019) Diastolic wall strain predicts progression from paroxysmal to persistent or permanent atrial fibrillation in structurally normal hearts. J Cardiol 74:339–346
9. Pathan F, D'Elia N, Nolan MT, Marwick TH, Negishi K (2017) Normal ranges of left atrial strain by speckle-tracking echocardiography: a systematic review and meta-analysis. J Am Soc Echocardiogr 30:59–70.e8
10. Mor-Avi V, Lang RM, Badano LP, Belohlavek M, Cardim NM, Derumeaux G, Galderisi M, Marwick T, Nagueh SF, Sengupta PP, Sicari R, Smiseth OA, Smulevitz B, Takeuchi M, Thomas JD, Vannan M, Voigt JU, Zamorano JL (2011) Current and evolving echocardiographic techniques for the quantitative evaluation of cardiac mechanics: ASE/EAE consensus statement on methodology and indications endorsed by the Japanese society of echocardiography. Eur J Echocardiogr 12:167–205
11. Miglioranza MH, Badano LP, Mihăilă S, Peluso D, Cucchini U, Soriani N, Iliceto S, Muraru D (2016) Physiologic determinants of left atrial longitudinal strain: a two-dimensional speckle-tracking and three-dimensional echocardiographic study in healthy volunteers. J Am Soc Echocardiogr 29:1023–1034.e3
12. Sugimoto T, Robinet S, Dulgheru R, Bernard A, Ilardi F, Contu L, Addetia K, Caballero L, Kacharava G, Athanassopoulos GD, Barone D, Baroni M, Cardim N, Hagendorff A, Hristova K, Lopez T, De La Morena G, Popescu BA, Penicka M, Ozyigit T, Rodrigo Carbonero JD, Van De Veire N, Von Bardeleben RS, Vinereanu D, Zamorano JL, Go YY, Marchetta S, Nchimi A, Rosca M, Calin A, Moonen M, Cimino S, Magne J, Cosyns B, Galli E, Donal E, Habib G, Esposito R, Galderisi M, Badano LP, Lang RM, Lancellotti P (2018) Echocardiographic reference ranges for normal left atrial function parameters: results from the EACVI NORRE study. Eur Heart J Cardiovasc Imaging 19:630–638
13. Kutty S, Padiyath A, Li L, Peng Q, Rangamani S, Schuster A, Danford DA (2013) Functional maturation of left and right atrial systolic and diastolic performance in infants, children, and adolescents. J Am Soc Echocardiogr 26:398–409.e2
14. Du Bois D, Du Bois EF (1916) Clinical calorimetry: tenth paper a formula to estimate the approximate surface area if height and weight be known. Arch Intern Med XVII:863–871
15. Porter TR, Shillcutt SK, Adams MS, Desjardins G, Glas KE, Olson JJ, Troughton RW (2015) Guidelines for the use of echocardiography as a monitor for therapeutic intervention in adults: a report from the American society of echocardiography. J Am Soc Echocardiogr 28:40–56
16. Lang RM, Badano LP, Mor-Avi V, Afilalo J, Armstrong A, Ernande L, Flachskampf FA, Foster E, Goldstein SA, Kuznetsova T, Lancellotti P, Muraru D, Picard MH, Rietzschel ER, Rudski L, Spencer KT, Tsang W, Voigt JU (2015) Recommendations for cardiac chamber quantification by echocardiography in adults: an update from the American society of echocardiography and the European association of cardiovascular imaging. J Am Soc Echocardiogr 28:1–39.e14
17. Lopez L, Colan SD, Frommelt PC, Ensing GJ, Kendall K, Younoszai AK, Lai WW, Geva T (2010) Recommendations for quantification methods during the performance of a pediatric echocardiogram: a report from the Pediatric Measurements Writing Group of the American Society of Echocardiography Pediatric and Congenital Heart Disease Council. J Am Soc Echocardiogr 23:465–495
18. Cole TJ, Green PJ (1992) Smoothing reference centile curves: The LMS method and penalized likelihood. Stat Med 11:1305–1319
19. Kobayashi T, Fuse S, Sakamoto N, Mikami M, Ogawa S, Hamaoka K, Arakaki Y, Nakamura T, Nagasawa H, Kato T, Jibiki T, Iwashima S, Yamakawa M, Ohkubo T, Shimoyama S, Aso K, Sato S, Saji T, Z Score Project Investigators (2016) A new Z score curve of the coronary arterial internal diameter using the lambda-mu-sigma method in a pediatric population. J Am Soc Echocardiogr 29:794–801.e29

20. Kanda Y (2013) Investigation of the freely available easy-to-use software "EZR" for medical statistics. Bone Marrow Transpl 48:452–458
21. Cantinotti M, Scalese M, Giordano R, Franchi E, Assanta N, Molinaro S, Iervasi G, Santoro G, Koestenberger M, Kutty S (2019) Left and right atrial strain in healthy caucasian children by two-dimensional speckle-tracking echocardiography. J Am Soc Echocardiogr 32:165–168.e3
22. Di Salvo G, Drago M, Pacileo G, Rea A, Carrozza M, Santoro G, Bigazzi MC, Caso P, Russo MG, Carminati M, Calabro R (2005) Atrial function after surgical and percutaneous closure of atrial septal defect: A strain rate imaging study. J Am Soc Echocardiogr 18:930–933
23. Shakti D, Friedman KG, Harrild DM, Gauvreau K, Geva T, Colan SD, Brown DW (2018) Left atrial size and function in patients with congenital aortic valve stenosis. Am J Cardiol 122:1541–1545
24. Kang SJ, Ha J, Hwang SJ, Kim HJ (2018) Long term outcomes of left atrial reservoir function in children with a history of Kawasaki disease. J Cardiovasc Ultrasound 26:26–32
25. Hope KD, Wang Y, Banerjee MM, Montero AE, Pandian NG, Banerjee A (2019) Left atrial mechanics in children: insights from new applications of strain imaging. Int J Cardiovasc Imaging 35:57–65
26. Khoo NS, Smallhorn JF, Kaneko S, Kutty S, Altamirano L, Tham EB (2013) The assessment of atrial function in single ventricle hearts from birth to Fontan: a speckle-tracking study by using strain and strain rate. J Am Soc Echocardiogr 26:756–764
27. Ishizaki U, Nagao M, Shiina Y, Inai K, Mori H, Takahashi T, Sakai S (2019) Global strain and dyssynchrony of the single ventricle predict adverse cardiac events after the Fontan procedure: analysis using feature-tracking cine magnetic resonance imaging. J Cardiol 73:163–170
28. Zhang C, Deng Y, Liu Y, Xu Y, Liu Y, Zhang L, Chen X, Xie M, Ge S (2018) Preclinical cardiovascular changes in children with obesity: a real-time 3-dimensional speckle tracking imaging study. PLoS ONE 13(10):e0205177
29. D'Ascenzi F, Anselmi F, Focardi M, Mondillo S (2018) Atrial enlargement in the athlete's heart: assessment of atrial function may help distinguish adaptive from pathologic remodeling. J Am Soc Echocardiogr 31:148–157
30. Genovese D, Singh A, Volpato V, Kruse E, Weinert L, Yamat M, Mor-Avi V, Addetia K, Lang RM (2018) Load dependency of left atrial strain in normal subjects. J Am Soc Echocardiogr 31:1221–1228
31. Burns AT, La Gerche A, D'hooge J, Macisaac AI, Prior DL (2010) Left ventricular strain and strain rate: characterization of the effect of load in human subjects. Eur J Echocardiogr 11:283–289
32. Vianna-Pinton R, Moreno CA, Baxter CM, Lee KS, Tsang TS, Appleton CP (2009) Two-dimensional speckle-tracking echocardiography of the left atrium: feasibility and regional contraction and relaxation differences in normal subjects. J Am Soc Echocardiogr 22:299–305
33. Okamatsu K, Takeuchi M, Nakai H, Nishikage T, Salgo IS, Husson S, Otsuji Y, Lang RM (2009) Effects of aging on left atrial function assessed by two-dimensional speckle tracking echocardiography. J Am Soc Echocardiogr 22:70–75
34. Sakata M, Hayabuchi Y, Inoue M, Onishi T, Kagami S (2013) Left atrial volume change throughout the cardiac cycle in children with congenital heart disease associated with increased pulmonary blood flow: evaluation using a novel left atrium-tracking method. Pediatr Cardiol 34:105–111
35. Rimbaş RC, Mihăilă S, Vinereanu D (2016) Sources of variation in assessing left atrial functions by 2D speckle-tracking echocardiography. Heart Vessels 31:370–381
36. Tanaka S, Noda T, Kawasaki M, Segawa T, Tsugita N, Fuseya T, Kubota T, Iwama M, Nishigaki K, Watanabe S, Minagawa T, Ohashi H, Minatoguchi S (2019) Relationship between electrical conduction and phasic left atrial function: P-wave signal-averaged electrocardiography and time-left atrial volume curve assessments using two-dimensional speckle-tracking echocardiography. Heart Vessels 34:1212–1220
37. de Waal K, Phad N, Boyle A (2018) Left atrium function and deformation in very preterm infants with and without volume load. Echocardiography 35:1818–1826
38. Sabatino J, Di SG, Prota C, Bucciarelli V, Josen M, Paredes J, Borrelli N, Sirico D, Prasad S, Indolfi C, Fraisse A, Daubeney PEF (2019) Left atrial strain to identify diastolic dysfunction in children with cardiomyopathies. J Clin Med 8(8):E1243
39. Cantinotti M, Lopez L (2013) Nomograms for blood flow and tissue Doppler velocities to evaluate diastolic function in children: a critical review. J Am Soc Echocardiogr 26:126–141
40. Cantinotti M, Giordano R, Scalese M, Murzi B, Assanta N, Spadoni I, Crocetti M, Marotta M, Molinaro S, Kutty S, Iervasi G (2016) Nomograms for mitral inflow Doppler and tissue Doppler velocities in Caucasian children. J Cardiol 68:288–299
41. Dallaire F, Slorach C, Hui W, Sarkola T, Friedberg MK, Bradley TJ, Jaeggi E, Dragulescu A, Har RLH, Cherney DZI, Mertens L (2015) Reference values for pulse wave doppler and tissue doppler imaging in pediatric echocardiography. Circ Cardiovasc Imaging 8:1–9
42. Masutani S, Saiki H, Kurishima C, Kuwata S, Tamura M, Senzaki H (2014) Assessment of ventricular relaxation and stiffness using early diastolic mitral annular and inflow velocities in pediatric patients with heart disease. Heart Vessels 29:825–833
43. Cameli M, Sparla S, Losito M, Righini FM, Menci D, Lisi M, D'Ascenzi F, Focardi M, Favilli R, Pierli C, Fineschi M, Mondillo S (2016) Correlation of left atrial strain and Doppler measurements with invasive measurement of left ventricular end-diastolic pressure in patients stratified for different values of ejection fraction. Echocardiography 33:398–405
44. Takahashi K, Nii M, Takigiku K, Toyono M, Iwashima S, Inoue N, Tanaka N, Matsui K, Shigemitsu S, Yamada M, Kobayashi M, Yazaki K, Itatani K, Shimizu T (2019) Development of suction force during early diastole from the left atrium to the left ventricle in infants, children, and adolescents. Heart Vessels 34:296–306
45. Hayashi S, Yamada H, Bando M, Saijo Y, Nishio S, Hirata Y, Klein AL, Sata M (2015) Optimal analysis of left atrial strain by speckle tracking echocardiography: P-wave versus R-wave trigger. Echocardiography 32:1241–1249
46. Ryan L (2019) Four papers on child growth modelling. Stat Med 38:3505–3506
47. Martinez-Millana A, Hulst JM, Boon M, Witters P, Fernandez-Llatas C, Asseiceira I, Calvo-Lerma J, Basagoiti I, Traver V, De Boeck K, Ribes-Koninckx C (2018) Optimisation of children z-score calculation based on new statistical techniques. PLoS ONE 13(12):e0208362

論文の要約

Normal reference values for left atrial strains and strain rates in school children assessed using two-dimensional speckle-tracking echocardiography

2D スペックルトラッキング法による正常小児の左房機能評価

背景　左房機能には左室収縮期に肺静脈から血流を受ける Reservoir 機能、左室拡張早期に左房から左室へ血液が移動する Conduit 機能、左室拡張末期に心房収縮により左房内血液を押し出す Contractile 機能の 3 つが存在する（図 1 ）。近年では 3Dスペックルトラッキングや CT または MRI を用いた左房解析が報告されている。しかし 2D スペックルトラッキング (2DSTE)法によるストレイン（ε）およびストレインレート（SR）の解析は、より簡便かつ時間分解能に優れており、各相毎の左房機能評価が可能で、成人の領域では左室機能障害を鋭敏に反映する早期指標として有用であると報告され、基準値もすでに確立している。しかし小児領域においては左房 ε および SR を用いた左房機能解析に関する報告は少ないうえに、成熟段階に伴う心拍数の変化、体格の変化が及ぼす各値への影響に関する検討が十分でない。このため本研究では、2DSTE 法を用い、正常小児における左房 ε（Reservoir ストレイン：εRS, Conduit ストレイン：εCD, Contractile ストレイン：εCT）および SR (positive SR :SR_{POS}, early negative SR :SR_{EN}, late negative SR :SR_{LN})の計測値から z スコアカーブを求め、成長による変化が各値に及ぼす影響を調べる目的で検討した。

方法　本研究は 2016 年 5 月から 2017 年 12 月の間、心雑音や胸痛および動悸などの循環器症状を主訴に来院した患者 153 名に対し、心スクリーニングを行い、器質的心疾患を認めた 13 名を除外した 140 名(年齢 6 歳から 16 歳まで)を対象とした。対象者に対し、Artida (CANON Medical Systems,Tochigi, Japan)を使用し、左室収縮能、従来のパルスドプラー法を用い左室拡張能の指標（E/A, E/e’）および左室流出路面積より一回拍出量を計測した。また、Biplane area length method 法により左房容積を求めた。さらに、左室機能との相関を調べる目的で M mode 法を用いて僧帽弁輪収縮期移動距離（mitral annular plane systolic excursion: MAPSE）を併せて計測した。その後、図 2 に示すように、汎用画像診断装置ワークステーション用プログラム(2D Cardiac Performance Analysis, TomTec Imaging system)を用い、左房ストレイン（ε）およびストレインレート（SR）を計測した。計測した各指標は lambda-mu-sigma (LMS) 法を用いて年齢、体表面積、心拍数それぞれを横軸に z スコア化した。体表面積は DuBois 法で求めた。

結果　左房解析の結果、画質不良ゆえ 28 名が解析困難であったため 112 名のデータを最終的に用い検討した。対象者の特徴およびエコーデータを表 1 ～ 3 に示す。各計測値に性差は認め

なかった。表4は、各εおよびSRと各種ドップラーパラメータおよび左房容積との相関を示す。E/AはSR_{LN}と弱い負の相関を示した。E/e'はεRSとεCDに負の相関を示したがいずれのSRにも相関を示さなかった。MAPSEはεRS, εCD, SR_{POS}にそれぞれ正の相関を認めた（P<0.01, r=0.36, 0.36, 0.32）。作成したz scoreカーブを図3に示す。年齢と体表面積に関しては、εおよびSR ともにほぼ横ばいあるいは軽度の下降スロープを描き、下降の程度はεよりもSRで顕著であった。一方、心拍数に関してはεCTをのぞくεおよびSR_{POS}はほとんど影響をうけず、ほぼ横ばいであったが、εCT ,SR_{EN}およびSR_{LN}は、高心拍数になるにつれカーブの上昇の傾向を認めた。検査者間および検査者内の再現性について表5に示す。いずれの指標も良好な再現性を認めた。

考察

本研究では、健常学童における左房εおよびSRのz scoreカーブを作成した。2DSTEの汎用画像診断装置ワークステーション用プログラムを用い、この年齢層における各指標について、年齢、体表面積および心拍数をもとにzスコアカーブを作成したのは本論文が最初である。また、過去の報告に西洋人と日本人のεおよびSRとの比較がないため、本研究は日本人の小児のみを対象として左房εおよびSRを検討した初めての報告となる。

過去の報告との比較

これまで、小児の領域における左房解析は、心房中隔欠損症[22]、大動脈弁狭窄症[23]ほか、左房拡大をきたす疾患の心機能障害を評価する指標として有用との報告[25]がされている。心房中隔欠損症では、Amplatzer septal occluderによるカテーテル治療と外科的閉鎖術の二つがあるが、術後遠隔期の比較では明らかに外科的閉鎖術のほうが、εRSおよびSRposともに低下しているとの報告がある。これは、術後切開線をめぐる心房筋の線維化という心房性不整脈発生の原因を反映していると考えられる。そして、低侵襲というだけでなく、心房機能の意味においても、適応のある心房中隔欠損症にはカテーテル治療を推奨する根拠となりうる。単に遺残短絡の有無という術後評価にとどまらずに心房機能を評価することが、小児から成人へ移行する際の長期管理の上で重要になってくるであろう。また、大動脈弁狭窄症においては、左室拡張末期圧上昇を反映し、εCTが顕著に上昇していると報告されている。先天性の場合、重症なほど出生後すぐにバルーン拡張術を施行するが、術後再狭窄に伴う左室機能評価の際に、左室拡張末期圧が推測できるとすれば、大変有用と考えられる。実際、e'/EをεRSで除した式で求めるnoninvasive LA stiffness($\%^{-1}$)という値は、左室拡張末期圧と良好な相関を示したとのデータがある。左房拡大をきたしうる左右シャントを有する疾患や心筋症の患者において従来のドップラー指標と組み合わせて活用することは、より精度の高い拡張能障害診断の一助となるであろう。また、小児の心筋症における左房機能を活用した報告では、εRS≧40.4%（感度98%、特異度99%）、SRpos≧$1.39s^{-1}$(感度88%、特異度90%)で肥大型心筋症、拡張型心筋症や拘束型心筋症といった心筋症から鑑別するカットオフ値としている。これは本研究のzスコアでいうとz 0またはz +1に相当する。今後実際の症例を計測しながらzスコアを当てはめて

検討する必要がある。さらに、健常人においてはアスリートに対する定期的な心モニタリングの報告[29]もある。アスリートは、突然死の予防からも心スクリーニングが欠かせないが、トレーニングによる酸素消費量の増大に伴い、循環血液量が増加し、心エコーでは左房拡大をみることが多い。この場合、拡張能障害に起因する左房拡大との鑑別において左房ストレインが有用であると報告されている。また、成人を対象にした MRI による検討ではあるが、肥満および 2 型糖尿病を合併した群では、コントロール群との比較において左房拡大や左室機能の有意差はないものの有意に左房ストレインの低下を認めた。さらに、MRI で計測した心外膜脂肪量および BMI に対し左房ストレインと負の相関を認めたと報告されている[#1]。収縮能が保たれた心不全を合併しやすい肥満の心スクリーニングにおいても左房機能は今後さらに注目される可能性がある。また、今回対象とした小児の年齢の範囲においては、成人の基準値（εRS 39%、εCD23%、εCT17%）と比較した場合[9]、z スコア上収縮期の指標である εRS および εCD はほぼ z ＝ 0 の位置にあるが、拡張期後期の指標である εCT に関しては、 z ＝＋ 1 .0 から＋ 2 .0 の位置であり、加齢による左室の stiffness の増大が拡張期後期の指標に影響したか、あるいは成人との心拍数の相違が一因と考えられる。逆に、収縮期および拡張早期の左房ストレインに関しては本研究の対象年齢ですでに成人と変わらない程度に成熟し安定していると考えてよいかもしれない。

本研究の結果解釈

パルスドップラー指標と本研究で得られた左房ストレイン値を比較すると、E/A および E/e’に関しては、全値との相関は本研究では得られなかった。これまでの研究で、ある程度の相関が示されているデータがある以上断定はできないが、本研究結果の全体的なばらつきの要因の一つにはパルスドップラー指標のもつ、角度依存性や容量依存性の問題が考えられる。また、A 波および e’の指標は顕著に心拍数と相関を示すことがわかっており[39]、成人の検討でも心拍数が 10 回／分上昇するごとに E/A は 0.5〜0.9 上昇するとの報告[#2]もある。本研究では鎮静をしていない、心拍数が一定と仮定できない小児が対象ゆえ、心拍数のゆらぎが影響した可能性がある。唯一関連のあった SR_{LN} は高心拍数による A 波への影響と相関したのかもしれない。また E/e’に関しては εCD および SR_{EN} との相関を期待したが、SR_{EN} との相関はなかった。心筋の収縮（または拡張）力を反映する SR よりも、ε は各心周期における左房の変化率をみているため、従来のドップラー指標に近似するは ε の方なのかもしれない。収縮期に焦点をあてれば、MAPSE は εRS および SRpos と相関がみられた。体表面積で補正した左房容量と 1 回拍出量において SR_{EN} が弱いながらも負の相関を示したことは、拡張早期に左室に流入する血液が体格的に少ないほうが、拡張早期の左房筋の収縮は速いという事実を示している。容量負荷のかかる心疾患の評価では、鋭敏に反応する指標として有用かもしれない。

ここで過去の研究と本研究の結果を踏まえ、左房 ε と SR のデータをどのように小児に適用するか提案してみたい。

左房ではなく左室機能を対象とした研究ではあるが、小児の心拍数との関連を調べた研究では、心拍数は各心周期における左室 ε と相関し、左室 SR に関しては拡張後期の左室 SR のみ影

響を与え、収縮期と拡張早期の左室 SR は相関しなかったと報告されている[#3]。高心拍数下では、今回の研究では、SR は ε に比べて良好な時間分解能ゆえ、とくに拡張期の指標で大いに心拍数の影響をうけた。心拍数と、収縮期・拡張早期・拡張後期それぞれの時間の相関を示した過去の報告によると[#3]、心拍数が 100 回／分を超えるまでは拡張早期時間は指数関数的に減少し、他は心拍数の増加に比例して時間の減少を認めている。このことは 100 回／分を超える高心拍領域では、心拍数 100 回／分より低い場合に比べ、拡張期における後期（心房収縮期）の占める割合が、高いことを示唆している。よって、本研究で対象にした小児の年齢においては心拍数では εCT の増加はなだらかな上昇にとどまったが、基本的には拡張期の指標は ε も SR も影響をうけると考えてデータを解釈すべきであろう。心拍数は、小児から成人への成長過程における一回心拍出量の増加に伴い減少するため、年齢や体格と元来密接な関係がある。よって年齢や体表面積の解釈には心拍数の影響が避けられない。ε と SR のどちらが評価に有用であるかの結論は本研究の範囲では収まらない今後の検討課題である。心拍数 100 回／分を超える領域の拡張早期および後期の指標に関しては、年齢や体表面積よりもまず心拍数をもとにしたグラフから求めた z スコアから判定していくとよいだろう。とくに、SR は時間分解能がよいため、今回の対象からは除外した 5 歳以下の高心拍数下ではより期待できる指標となりうるが、この点に関しても今後の検討課題である。

小児の左房機能解析における今後の応用について

拡張能評価には左室流入血流速度波形（拡張早期最大流速 E 波、心房収縮期最大流速 A 波)、僧帽弁輪組織パルスドップラー法（僧帽弁輪収縮期運動速度 e'、僧帽弁輪拡張早期運動速度 a'、僧帽弁輪心房収縮期運動速度 s ')、肺静脈血流波形、Tei インデックスがあり、小児の心エコーでもこれらを成人同様に駆使して評価している。しかし、小児の左室拡張能障害の評価に関しては、成人のアルゴリズムを小児にそのまま適応してよいのかという議論がある。現状では、スペックルトラッキング法を用いる心機能解析に関しては、左房よりも先にデータが蓄積されている左室に関してすら小児科領域では臨床に普及しているとは言えない。また、これまでは左室解析用のソフトを代用していたが、近年本研究で使用した左房解析のためのソフトが開発され、基準値の集積が始まったばかりである。本研究で得られた ε および SR の値は、従来の拡張能指標と十分な相関を示さなかった。しかし、従来の指標が左室拡張末期圧を反映せず[42]、左室収縮能に影響を受ける[43]指標だとすれば、今回のスペックルトラッキング法を用いた左房機能解析は年齢、体表面積、心拍数といった因子の考慮が必要ながらも、従来の指標に加えることにより、より精度の高い左室拡張能評価を実現する可能性がある。そのためには、これまでの研究で行われているように、観血的あるいは非観血的な手法で左房圧近似のデータを求め、あるいは臨床症状との相関を示していくことが重要と考える。実際の小児への応用に関しては２つ議論すべき点がある。１点目は計測のタイミングに関して、Ｐトリガー法とＲトリガー法がある。今回はＰトリガー法を用いたが、心拍数の早い小児にはＰトリガー法のほうが、εCT が明瞭に描出できるため推奨される。２点目はスペックルトラッキング心エコー法による計測に関して、２Ｄと３Ｄがある。近年では３Ｄを用いた研究により２Ｄに比べて良

好な再現性および正確性が指摘される上、２Ｄでは計測できない Circumferential ストレインが計測できる利点もある。しかし、息止めの困難な小児では３Ｄ計測が困難なケースも存在するほか、２Ｄは３Ｄにくらべ優れた時間分解能ゆえ、高心拍数の小児では依然として有用と考えられる。

本研究の限界

本研究の限界について述べる。まず 1 点目は、z スコア表の作成において対象者数が少ないことはサンプリングバイアスを引き起こす危険がある。しかし、当研究は後方視研究であり、データの不ぞろい、描出画像の精度などの影響で、サンプル数が少なくなってしまった。また、本研究の対象外とした 6 歳未満の小児においても十分な症例数を用いた同様の検討が今後必要であろう。2 点目に、小児を対象としたため、呼気終末での画像取得が困難な症例が含まれていたことである。左房機能は呼吸に影響するため、これを克服するため 3 心拍の平均を値として用いるようにした。3 点目にコントロール群の抽出方法であるが、心スクリーニングの時点で正常心であった対象者を抽出したが、完全には代謝性疾患の素因を有するものを除外できたとは断言できない。4 点目には、左房機能解析のための画像取得にある一定の技術を要することである。画像の精度は Region of interest や Frame rate の設定や、グレースケールの設定、被検者の体位などが大きく影響する。鎮静が得られない年齢における小児では、こうした準備が時に困難であることは否めない。しかし３D に比べ、２D では左房に焦点を当てた四腔像の記録だけであとはオフラインで解析できるため、日ごろのスクリーニングに特別な画像を加える必要がないという点で、今後小児における心機能評価として普及する可能性を十分に秘めていると考えられる。最後に、一般的には心エコー検査装置の世界市場では Philips, GE, CANON の 3 社でスペックルトラッキング解析が行われているが、この 3 社では得られるストレイン値にばらつきがあることが指摘されており[#4]、本研究では汎用画像診断装置ワークステーション用プログラムを用いて解析を行った。しかし実際にはこの 2Dsoftware (2D Cardiac Performance Analysis, TomTec Imaging system, Munich, Germany)をもっている小児科は非常に少ないのが現状であり、主流 3 社の値と本ソフトウェアで得られた解析値との相関を検討することは、本研究で得られた z スコア値を臨床応用するための重要な今後の課題であろう。

結語　ε は本研究の対象年齢においてはほぼ横ばいであったが、拡張期を示す指標に関しては、とくに SR において心拍数が影響することが考えられた。2DSTE 法は小児においても簡便で再現性のある検査であり、左房機能評価においては ε と SR は同時に評価し解釈することが重要である。